

## A Three-Dimensional Nodal Diffusion Code Based on the AFEN Methodology

Ser Gi Hong, Nam Zin Cho, and Jae Man Noh

Korea Advanced Institute of Science and Technology

(Received August 31, 1995)

### 해석함수전개 노달방법에 기초한 3차원 노달확산 코드

홍서기 · 조남진 · 노재만

한국과학기술원

(1995. 8. 31 접수)

#### Abstract

In this paper, a new three-dimensional nodal diffusion code which is based on the AFEN methodology is described and tested. The method expands the homogeneous flux within a node in terms of eighteen analytic basis functions satisfying the diffusion equation at any point of the node. And the nodal coupling equations are derived such that nodal balance, current continuity and leakage balance within an infinitesimally small box around the edge are satisfied. To verify its accuracy, the code was applied to the well-known static LMW benchmark problem and a small core benchmark problem that has the same material properties as the three-dimensional IAEA benchmark problem, and compared with two other codes (QUANDRY, VENTURE). The results show that the code provides good accuracy both in the power distribution and in the effective multiplication factor.

#### 요 약

해석함수전개 노달방법에 기초한 새로운 3차원 노달확산 코드가 개발되었다. 이 방법은 균질화된 노드내의 해를 노드내에서 중성자확산방정식을 만족하는 해석적인 18개의 기저함수들과 1개의 상수로 전개한 후 노달연관방정식을 노드에 대한 중성자의 균형, 경계면에서의 중성자류의 연속, 모서리주위의 무한히 작은 체적소에 대한 중성자누출의 균형이 만족되도록 유도한다. 이 코드의 정확성을 검증하기 위해 잘 알려진 LMW표준문제와 IAEA 3차원 문제와 동일한 물질을 가지는 작은 노심문제에 적용하여 QUANDRY코드 및 VENTURE코드의 결과와 비교하였다. 계산결과들은 본 연구에서 개발된 코드가 출력분포 및 유효증배계수를 매우 정확하게 예측함을 보여준다.

#### 1. Introduction

In analyzing a nuclear reactor, the nodal methods

are usually used due to their higher accuracy and much shorter computing time. In this paper, a new three-dimensional nodal code[1] based on the AFEN

method is described and tested. In most modern nodal methods, the multidimensional diffusion equation is decoupled into several one-dimensional equations by the transverse integration procedure and the resultant transverse leakage terms are approximated by a parabolic fit. Therefore, these methods have some limitations. But the AFEN method expands the solution in terms of analytic basis functions satisfying the diffusion equation in a node and directly solves the resultant nodal coupling equations without the transverse integration procedure. Therefore, the AFEN method gives very accurate solutions even near the nodal interface of strong material discontinuity. The two-dimensional results of the method have been reported in several papers[2-5].

The methodology of this three-dimensional AFEN code parallels the two-dimensional case. The nodal unknowns are one node average flux, six interface fluxes and twelve edge fluxes per node per group. To represent these nodal unknowns, the homogeneous flux is expanded in terms of eighteen analytic basis functions satisfying the diffusion equation and one additional constant. The expansion coefficients are then represented by the nodal unknowns. Therefore, nineteen equations per node per group are required. The equation for the node average fluxes is the nodal balance equation and the equation for the interface fluxes is the current continuity equation. The equation for the edge fluxes is obtained by equating the sum of the net leakages within an infinitesimally small box around the edge to zero. This means that the neutron balance is equal to the leakage balance if this box is infinitesimally small. Since only four nodes around the edge are coupled by the edge balance equation, the nodal formulation is simplified while the directional symmetry of the formulation is preserved.

## 2. Theory and Methodology

The starting equation is the three-dimensional static diffusion equation for homogenized cubic node  $n$ :

$$-D\nabla^2 \bar{\phi}^n(x, y, z) + \Sigma^n \bar{\phi}^n(x, y, z) = \frac{1}{k_{eff}} \nu \Sigma_f^n \bar{\phi}^n(x, y, z). \quad (1)$$

If  $\lambda_g^n$  are defined as the eigenvalues of the matrix  $(D^n)^{-1}[\Sigma^n - \frac{1}{k_{eff}} \nu \Sigma_f^n]$  and matrix  $R^n$  as the  $2 \times 2$  matrix with corresponding eigenvectors, and if a new unknown  $\xi$  is defined by the relation

$$\bar{\phi}^n(x, y, z) = (R^n)^{-1} \xi^n(x, y, z), \quad (2)$$

Eq.(1) is decoupled into "mode-group" partial differential equations as follows:

$$\nabla^2 \xi_g^n(x, y, z) - \lambda_g^n \xi_g^n(x, y, z) = 0, \quad g = 1, 2. \quad (3)$$

Here,  $g$  is the "mode-group" index. Then, the solution of Eq.(3) is expanded in terms of eighteen analytic basis functions and an additional term as follows:

$$\begin{aligned} \xi_g^n(x, y, z) = & C_g^n + \sum_u \{A_{g0}^u SN x_g^u u + A_{g1}^u CS x_g^u u\} \\ & + \sum_{u,v:u \neq v} \{A_{g00}^{uv} SN \frac{\sqrt{2}}{2} x_g^u u SN \frac{\sqrt{2}}{2} x_g^v v \\ & + A_{g01}^{uv} SN \frac{\sqrt{2}}{2} x_g^u u CS \frac{\sqrt{2}}{2} x_g^v v \\ & + A_{g10}^{uv} CS \frac{\sqrt{2}}{2} x_g^u u SN \frac{\sqrt{2}}{2} x_g^v v \\ & + A_{g11}^{uv} CS \frac{\sqrt{2}}{2} x_g^u u CS \frac{\sqrt{2}}{2} x_g^v v\} \end{aligned} \quad (4)$$

where

$$\begin{aligned} x_g^n &= (|\lambda_g^n|)^{1/2} \\ SN x_g^n u &= \begin{cases} \sinh x_g^n u, & \lambda_g^n > 0 \\ \sin x_g^n u, & \lambda_g^n < 0 \end{cases} \\ CS x_g^n u &= \begin{cases} \cosh x_g^n u, & \lambda_g^n > 0 \\ \cos x_g^n u, & \lambda_g^n < 0 \end{cases} \\ u &= x, y, z. \end{aligned} \quad (5)$$

The above nineteen coefficients can be easily expressed in terms of nineteen nodal unknowns and used in later formulation. For example,

$$A_{g00}^{xy} = \frac{\delta \xi_{g11}^{n,xy} + \delta \xi_{g00}^{n,xy} - \delta \xi_{g01}^{n,xy} - \delta \xi_{g10}^{n,xy}}{4 SN \frac{\sqrt{2}}{4} x_g^n h_x SN \frac{\sqrt{2}}{4} x_g^n h_y} \quad (6)$$

where

$$\delta \xi_{gij}^{n,xy} = \xi_{gij}^{n,xy} + \bar{\xi}_g^n - (\xi_{g,i}^{n,x} + \xi_{g,j}^{n,y})$$

The nodal coupling equations are then derived. The first nodal coupling equation imposed on the nodal unknowns is the nodal balance equation that is derived by integrating Eq.(1) over the node :

$$\begin{aligned} & \left\{ \sum_u 2 \frac{D}{h_u^2} \langle (I + \alpha^u)(\Lambda_1^u - \gamma_1^u) - \alpha^u(\Lambda_2^u - \gamma_2^u) \rangle + \Sigma \right\} \vec{\phi}_{ijk} = \\ & \left\{ \sum_u \frac{D}{h_u^2} \langle (I + \alpha^u)(\Lambda_1^u - \gamma_1^u) \right. \\ & \quad \left. - \alpha^u(\Lambda_2^u - \gamma_2^u) \rangle \right\} \vec{\phi}_{(u)JK}^{u+1/K} + \vec{\phi}_{(u)JK}^u \\ & + \left\{ \sum_u \frac{D}{h_u^2} \sum_{v \neq u} \langle \alpha^v(\Lambda_2^v - \Lambda_1^v + \gamma_1^v - \gamma_2^v) \rangle \right\} \vec{\phi}_{ijk} \\ & + \frac{1}{2} \left\{ \sum_{p,q=0,1} \vec{\phi}_{(u)+p(K)+q(K)}^{uv} - 2(\vec{\phi}_{(u)+1/K}^v + \vec{\phi}_{(u)/K}^v) \right\} \end{aligned} \quad (7)$$

where the matrices  $\alpha$ ,  $\beta$ ,  $r$ ,  $\Lambda$  are all diagonal matrices and the symbol  $\langle \rangle$  on a matrix denotes similarity transformation by  $R$ . In Eq.(7),  $I(u)$  denotes mesh index of  $u$ -direction and  $J, K$  denote mesh indices of the other directions. Second, the equation for the surface flux is derived by imposing continuity on the interface currents at node interfaces. The equation for the  $x$ -direction interface flux is given as follows :

$$\begin{aligned} & \left\{ \frac{D}{h_x} \langle \alpha^x \gamma_2^x \rangle - \langle (I + \alpha^x) \gamma_1^x \rangle \right\} \vec{\phi}_{i-1,jk}^x \\ & + \left\{ \frac{D}{h_x} \langle (I + \alpha^x) \Lambda_1^x \rangle - \langle \alpha^x \Lambda_2^x \rangle \right\} \vec{\phi}_{ijk}^x \\ & + \left\{ \frac{D}{h_x} \langle (I + \alpha^x) \Lambda_1^x \rangle - \langle \alpha^x \Lambda_2^x \rangle \right\} \vec{\phi}_{ijk}^x \\ & + \left\{ \frac{D}{h_x} \langle \alpha^x \gamma_2^x \rangle - \langle (I + \alpha^x) \gamma_1^x \rangle \right\} \vec{\phi}_{i+1,jk}^x = \vec{P}_{ijk}^x \end{aligned} \quad (8)$$

where  $\vec{P}_{ijk}^x$  contains the node average flux terms, the  $y$ -direction interface flux terms, the  $z$ -direction interface flux terms, and the edge flux terms of the two nodes.

Finally, the edge balance equation for the edge average flux is derived by considering the neutron leakage balance within an infinitesimally small box in two directions (e.g.,  $x, y$ ) with height  $h_x$  around the edge that is shared by four adjacent nodes. This formulation leads to the five block matrix equation for the edge average fluxes. The resulting equation is not presented here to save space.

The complete nodal coupling equations for all nodal unknowns are now established. These nodal

coupling equations are solved by the conventional source iteration method that consists of two levels of iterative schemes (i.e., inner iteration and outer iteration), similarly as in the two-dimensional case.

### 3. Application and Results

For verification of our three-dimensional nodal diffusion code AFEN, the code was firstly applied to the well-known LMW benchmark problem[6] (static version) and the results are compared with those of other two codes QUANDRY[7] and VENTURE[8]. The configuration of the benchmark problem is shown in Fig. 1 and the cross sections in Table 1. This benchmark problem is a simplified LWR. The reactor has a two-zone core containing 77 fuel assemblies with width of 20cm. The core is reflected both radially and axially by 20cm of water and the active core height is 160cm. Five control rods are parked in the upper axial reflector, and four control rods are inserted from the upper reflector to the axial midplane of the core.

The results show that the AFEN code improves accuracy both in the power distribution and in the core criticality. Fig. 2 shows the power distribution in

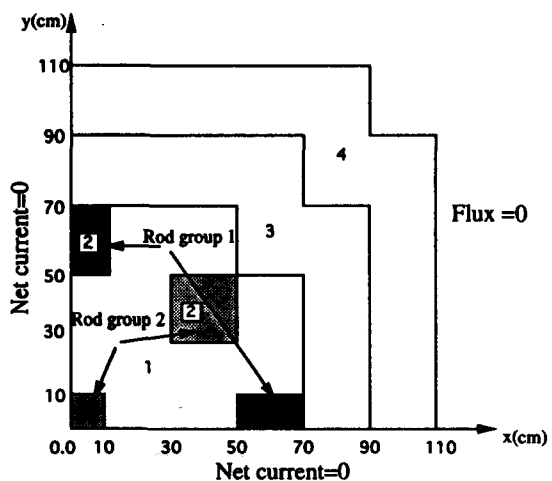


Fig. 1a. Quadrant of Reactor Horizontal Cross Section of the LMW Benchmark Problem

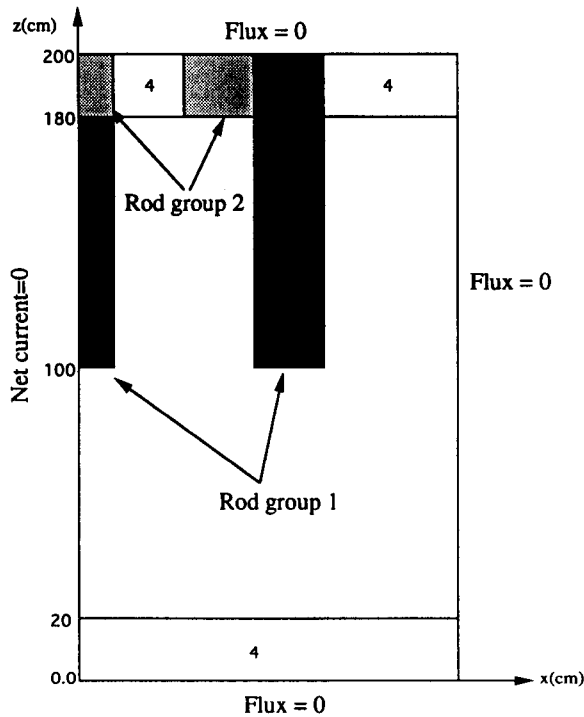


Fig. 1b. Vertical Cross Section

the 9th plane where the maximum error occurs in the active core region. Fig. 3 shows the assembly power density distribution. In this calculation, a uniform 20cm mesh in both radial and axial directions was used in AFEN and QUANDRY. The result of the VENTURE fine mesh calculation with a 1cm radial mesh and a 2cm axial mesh is used as reference solution. The maximum error in nodal power occurs at

a node in the upper axial reflector and is less than 1.13%. The maximum error in assembly power density occurs in the outermost assemblies and is less than 0.1%. The computing times in AFEN code and VENTURE code are given in Table 2.

Secondly, the code was applied to a small core problem that has the same material properties as the IAEA-3D benchmark problem. The benchmark problem was selected to provide a severe test for the capabilities of the code against the reliable reference solution (fine mesh VENTURE calculation). In this benchmark problem, the reactor consists of a two-zone core containing 45 fuel assemblies with width of

$k_{eff}$		0.3835	0.1925
		0.28	0.11
VENTURE	0.99960		
AFEN	error 0.004	0.5661	0.4399
QUANDRY	error 0.014	0.32	0.33
		0.7136	0.6258
		0.20	0.28
		0.4803	0.3110
		0.32	0.35
		0.7886	0.7461
		0.22	0.21
		0.6397	0.4702
		0.17	0.38
		0.3179	0.49

x.xxxx VENTURE power

x.xx AFEN error(%)

$$\text{Error} = \frac{\text{AFEN power} - \text{VENTURE power}}{\text{VENTURE power}} \times 100 (\%)$$

Shaded node : rodded assembly

Fig. 2. Nodal Power Distribution at 9th Plane for the LMW Benchmark Problem

Table 1. Macroscopic Cross Sections ( $\text{cm}^{-1}$ ) for the LMW Benchmark Problem

Composition	Group, g	$D_g$	$\Sigma_{ag}$	$\nu\Sigma_{fg}$	$\Sigma_{21}$
1	1	1.423913	0.01040206	0.006477691	0.0175555
	2	0.356306	0.08766217	0.112732800	
2	1	1.423913	0.01095206	0.006477690	0.0175555
	2	0.356306	0.09146217	0.112732800	
3	1	1.425611	0.01099263	0.007503284	0.0171776
	2	0.350574	0.09925634	0.137800400	
4	1	1.634227	0.002660573	0.000000000	0.0275969
	2	0.264002	0.049363510	0.000000000	

x.xxxx VENTURE power density				
x.xx	AFEN error(%)		0.8583	0.4329
x.xx	QUANDRY error(%)		0.04	-0.10
			0.44	0.21
		1.1231	0.9802	0.6260
		0.04	0.06	0.00
		-0.04	0.15	0.56
	1.5911	1.3970	1.0837	0.7072
	-0.06	-0.03	0.01	0.08
	-0.25	-0.19	-0.03	0.16
1.5559	1.6563	1.4414	0.9804	0.7257
-0.05	-0.07	-0.05	0.04	0.10
-0.27	-0.28	-0.24	-0.04	0.13

Fig. 3. Assembly Power Density Distribution

Table 2. Comparison of Computing Times (SUN SPARC-10)

Codes	AFEN*	VENTURE
Number of nodes	350	121000
Computing time (min)	6.58	797.50

\* No acceleration schemes used.

20cm. The severity of this benchmark problem is due to the nine control rods that are fully parked into the core. In this benchmark problem, the gradient of thermal flux is very steep near control rod assemblies. This fact is attributed to small core size and control rod assemblies. The configuration of the benchmark problem is given in Fig. 4 and the cross sections in Table 3. As in the previous benchmark problem, the

numerical results show that AFEN estimates accurately the power distribution and the core criticality. Figs. 5, 6 and 7 show nodal power distributions at the 2nd, 3rd and 4th planes, respectively. And Fig. 8 shows the assembly power density distribution. For this benchmark problem, the maximum error in the nodal power is 0.58% and the maximum error in the assembly power density is 0.45%. In this calculation, a uniform 20cm mesh in both radial and axial directions was used in AFEN. The result of the VENTURE fine mesh calculation with a 2/3cm radial mesh and a 2/3cm axial mesh is used as the reference solution. The computing times for this benchmark problem are given in Table 4.

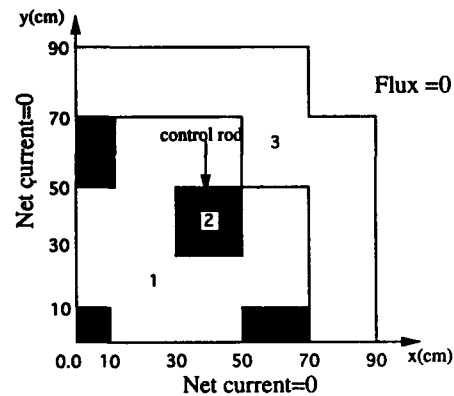


Fig. 4a. Quadrant of Reactor Horizontal Cross Section of the LMW Benchmark Problem

Table 3. Macroscopic Cross Sections ( $\text{cm}^{-1}$ ) for the Small Core Problem

Composition	Group, g	$D_g$	$\Sigma_{ag}$	$\nu\Sigma_{fg}$	$\Sigma_{21}$
1	1	1.5	0.010	0.000	0.02
	2	0.4	0.080	0.135	
2	1	1.5	0.010	0.000	
	2	0.4	0.130	0.135	
3	1	2.0	0.000	0.000	0.04
	2	0.3	0.010	0.000	
4	1	2.0	0.000	0.000	0.04
	2	0.3	0.055	0.000	

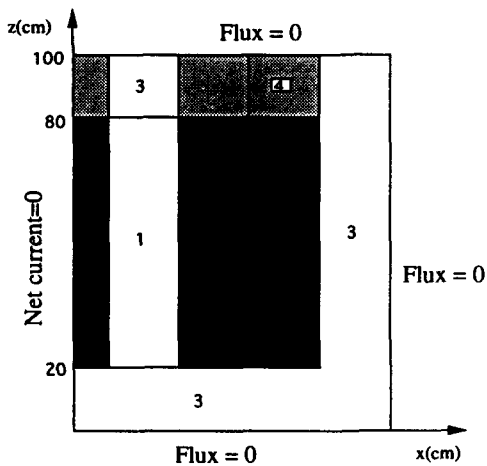


Fig. 4b. Vertical Cross Section

$k_{eff}$			
VENTURE	0.955247	0.4106	0.4006
AFEN error	0.0187	0.33	0.46
	1.7043	1.1740	0.5807
	0.48	0.18	-0.08
	0.9395	1.7266	1.3663
	0.37	0.24	-0.16
			0.3534
			-0.09

x.xxxx VENTURE power

x.xx AFEN error(%)

$$\text{Error} = \frac{\text{AFEN power} - \text{VENTURE power}}{\text{VENTURE power}} \times 100 (\%)$$

Shaded node : rodged assembly

Fig. 4. Nodal Power Distribution at 2nd Plane for the Small Core Benchmark Problem

			0.5567	0.5274
			0.31	0.23
	2.1825	1.5118	0.7567	
	0.18	-0.14	-0.38	
1.2714	2.2227	1.7533	0.4798	
0.40	-0.04	-0.51	-0.15	

Fig. 6. Nodal Power Distribution at 3rd Plane

			0.4564	0.4210
			0.46	0.20
	1.7501	1.2149	0.6075	
	0.19	-0.14	-0.38	
1.0411	1.7859	1.4067	0.3917	
0.58	-0.04	-0.55	0.02	

Fig. 7. Nodal Power Distribution at 4th Plane

			0.2847	0.2698
			0.36	0.29
	1.1273	0.7801	0.3889	
	0.28	-0.04	-0.29	
0.6504	1.1470	0.9014	0.2449	
0.45	0.04	-0.42	-0.07	

x.xxxx VENTURE power density

x.xx AFEN error(%)

Fig. 8. Assembly Power Density Distribution

Table 4. Comparison of Computing Times (SUN SPARC2)

Codes	AFEN*	VENTURE
Number of nodes	120	2733750
Computing time (min)	1.25	5406.50

\* No acceleration schemes used.

#### 4. Conclusions

In this paper, a new three-dimensional nodal diffusion code that is based on the AFEN methodology was described and tested. The AFEN code was developed to accurately analyze the three-dimensional reactor core. To test its accuracy and applicability to practical problems, the code was applied to the well-known LMW benchmark problem that models an LWR. The numerical results show that the code provides very accurate solutions in the nodal power distribution and in the core effective multiplication

factor in comparison with the VENTURE fine mesh calculation, while the QUANDRY code provides less accurate solution than AFEN over the whole region. In addition to the LMW benchmark problem, the code was applied to a small core problem that has the same material properties as the IAEA-3D benchmark problem for a severe test. In spite of the severity of the benchmark problem, the results indicate that AFEN provides very accurate solution. In virtue of the good accuracy, it is expected that the new code can be effectively used to analyze realistic reactor cores.

### References

1. S.G. Hong, N.Z. Cho and J.M. Noh, "Development of a Three-Dimensional Nodal Diffusion Code Based on the AFEN Methodology," *Proc. Korean Nuclear Society Spring Mtg.*, vol. 1, pp. 77–82, Ulsan, Korea, May 1995, Korean Nuclear Society (1995).
2. J.M. Noh and N.Z. Cho, "A New Approach of Analytic Basis Function Expansion to Neutron Diffusion Nodal Calculation," *Nucl. Sci. Eng.*, **116**, 165–180 (1994).
3. J.M. Noh and N.Z. Cho, "A New Nodal Method: Approach of Analytic Basis Function Expansion," *Proc. Korean Nuclear Society Spring Mtg.*, Kwangju, Korea, May 21–22, 1993, p. 13, Korean Nuclear Society (1993).
4. N.Z. Cho and J.M. Noh, "Analytic Function Expansion Nodal Method for Hexagonal Geometry," *Nucl. Sci. Eng.*, **121**, 245–253 (1995).
5. N.Z. Cho and S.G. Hong, "Mathematical Adjoint Solution to Analytic Function Expansion Nodal (AFEN) Method," *Journal of the Korean Nuclear Society*, vol. 27, pp. 374–384 (1995).
6. S. Langenbuch, W. Maurer, and W. Werner, "Coarse-Mesh Flux-Expansion Method for the Analysis of Space-Time Effects in Large Light Water Reactor Cores," *Nucl. Sci. Eng.*, **63**, 437–456 (1977).
7. K.S. Smith, "An Analytic Nodal Method for Solving the two-Group, Multidimensional, Static and Transient Neutron Diffusion Equation," Nuclear Engineering Thesis, Massachusetts Institute of Technology (1979).
8. D.R. Vondy et al., "VENTURE: A Code Block for Solving Multigroup Neutronic Problems Applying the Finite Difference Diffusion Theory Approximation to Neutron Transport-Version II," ORNL-5062/R1, Oak Ridge National Laboratory (1977).
9. Benchmark Problem Book, ANL-7416 Suppl. 2, Argonne National Laboratory, Argonne Code Center (1977).